PROCEEDINGS OF SPIE

SPIEDigitalLibrary.org/conference-proceedings-of-spie

Spectroscopy: a new route towards critical-dimension metrology of the cavity etch of nanosheet transistors

Bogdanowicz, J., Oniki, Y., Kenis, K., Muraki, Y., Nuytten, T., et al.

J. Bogdanowicz, Y. Oniki, K. Kenis, Y. Muraki, T. Nuytten, S. Sergeant, A. Franquet, V. Spampinato, T. Conard, I. Hoflijk, J. Meersschaut, N. Claessens, A. Moussa, D. Van Den Heuvel, J. Hung, R. Koret, A.-L. Charley, P. Leray, "Spectroscopy: a new route towards critical-dimension metrology of the cavity etch of nanosheet transistors," Proc. SPIE 11611, Metrology, Inspection, and Process Control for Semiconductor Manufacturing XXXV, 116111Q (22 February 2021); doi: 10.1117/12.2581800

SPIE.

Event: SPIE Advanced Lithography, 2021, Online Only

Downloaded From: https://www.spiedigitallibrary.org/conference-proceedings-of-spie on 23 Feb 2021 Terms of Use: https://www.spiedigitallibrary.org/terms-of-use

Spectroscopy: a new route towards critical-dimension metrology of the cavity etch of nanosheet transistors

J. Bogdanowicz*[a], Y. Oniki [a], K. Kenis [a], Y. Muraki [b], T. Nuytten [a], S. Sergeant [a], A. Franquet [a], V. Spampinato [a], T. Conard [a], I. Hoflijk [a], J. Meersschaut [a], N. Claessens [a,c], A. Moussa [a], D. Van den Heuvel [a], J. Hung [d], R. Koret [d], A.-L. Charley [a], P. Leray [a]

[a]Imec, Kapeldreef 75, 3001 Leuven, Belgium; [b]TEL Technology Solutions Ltd., Mitsuzawa 650, Hosaka-cho, Nirasaki, Japan 400-0192; [c]KULeuven, Dep. of Physics and Astronomy, C 200-D, 3001 Leuven, Belgium; [d]Nova Measuring Instruments Ltd., Israel

ABSTRACT

The processing of gate all-around Si transistors requires to isolate vertically stacked nanometer-thick Si sheets or wires. For this purpose, the SiGe layers of a SiGe/Si superlattice are etched selectively and laterally in a process step commonly called *cavity etch*[1,2]. Controlling the quantity of etched SiGe material, i.e. *the cavity depth*, is critical for optimal device performance. Unfortunately, this critical dimension (CD) can only be measured by time-consuming cross-sectional electron microscopy, which results in limited statistics and hence control of the cavity depth across wafers and batches. As a first step towards the development of fast inline cavity depth measurements, this work evaluates the sensitivity to cavity depth of conventional CD metrology and alternative top-down spectroscopic techniques on samples with cavity depths ranging from 0 to 30 nm. As we show, while optical CD scatterometry remains a technique of choice thanks to its high throughput and sensitivity, Raman and Energy-Dispersive X-ray spectroscopies also show very promising results owing to their simple sensitivity to the remaining SiGe volume. Finally, Secondary Ion Mass Spectrometry offers unique cavity profiling capabilities with a very high sensitivity down to SiGe residues, despite being time-consuming and destructive.

Keywords: cavity etch, lateral recess, critical dimension, inline metrology, Raman spectroscopy, Energy dispersive X-ray spectroscopy, X-ray photoelectron spectroscopy, Secondary ion mass spectrometry

1. INTRODUCTION

Novel gate-all-around devices like nanosheet, forksheet and ultimately Complementary Field-Effect Transistors (FETs) are due to replace today's finFETs as they offer both an enhanced electrostatic control and a reduced footprint[1]. Common to the processing of these different devices is the selective lateral recess, also called cavity etch, of the SiGe layers of a vertical Si/SiGe superlattice, to isolate the future vertically stacked Si channels[2]. The depth of these cavities is of paramount importance as it defines the dimensions of the inner spacer and hence the final gate capacitance[3]. However, this critical dimension (CD) can today only be determined by cross-sectional electron microscopy. Besides being time-consuming and destructive, this type of metrology only offers a very limited sampling e.g. across a wafer.

In this work, we evaluate the capabilities of conventional CD metrology and alternative spectroscopic techniques for fast inline cavity depth measurements on samples etched by a gas-phase isotropic dry etch process[2,4,5] and presenting cavity depths ranging from 0 to 30 nm. After describing our sample set in Section 2, we demonstrate in Section 3 that conventional techniques such as Scanning Electron Microscopy (SEM) and Atomic Force Microscopy (AFM) provide limited to no information about this buried CD. As we further show, Optical CD (OCD) scatterometry has a high sensitivity to the cavity depth. However, the unique reconstruction of the full device without correlations between the many geometrical parameters remains a challenge[6]. Finally, in Section 4, we demonstrate the capabilities of various top-down spectroscopic techniques, namely Energy-Dispersive X-ray Spectroscopy (EDX), Raman spectroscopy, X-ray Photoelectron Spectroscopy (XPS) and Secondary Ion Mass Spectrometry (SIMS). We show that these four techniques simply provide a measurement of the SiGe volume under the incident beam and hence contain sensitive information about the cavity depth. We conclude that Raman and EDX spectroscopies are very promising techniques for fast inline and precise cavity depth measurements. SIMS and XPS also do show interesting sensitivity to the cavity depth but they are inherently slower and/or destructive, hence less suited for inline metrology. Nevertheless, SIMS offers cavity profiling capabilities as well as a unique lower limit of detection and might remain a critically relevant technique e.g. in case of SiGe residue measurements.

*janusz.bogdanowicz@imec.be; https://www.imec-int.com/en

Metrology, Inspection, and Process Control for Semiconductor Manufacturing XXXV,
edited by Ofer Adan, John C. Robinson, Proc. of SPIE Vol. 11611, 116111Q
© 2021 SPIE · CCC code: 0277-786X/21/$21 · doi: 10.1117/12.2581800

Downloaded From: https://www.spiedigitallibrary.org/conference-proceedings-of-spie on 23 Feb 2021
Terms of Use: https://www.spiedigitallibrary.org/terms-of-use

2. EXPERIMENTAL

The aim of this paper is to evaluate the sensitivity of various techniques to cavity depth. For this purpose, we have processed four identical simplified nanosheet samples (Fig. 1). These samples consist of an array of ~100-nm wide fins comprising a 6-layer $Si_{75}Ge_{25}$/Si superlattice covered with a ~100-nm thick SiO_2/SiN/SiO_2 hard mask[5]. The nominal thicknesses of the different layers in the superlattice are all of 9 nm. The samples were etched by a gas-phase isotropic dry etch process[2,4,5] for four different times, leading to cavity depths ranging from 0 to 28.7 nm as illustrated in Figs 1(a) to (d). As also indicated, this corresponds to a reduction in SiGe volume of up to 46%, considering a constant width of 120 nm at the SiGe/Si superlattice. These samples were used for evaluation of top-down spectroscopic techniques (Section 4).
Besides these 4 samples, another set of 2 full wafers with identical processing and respective nominal cavity depths of 15 nm and 30 nm were used for evaluation of conventional CD metrology techniques (Section 3).

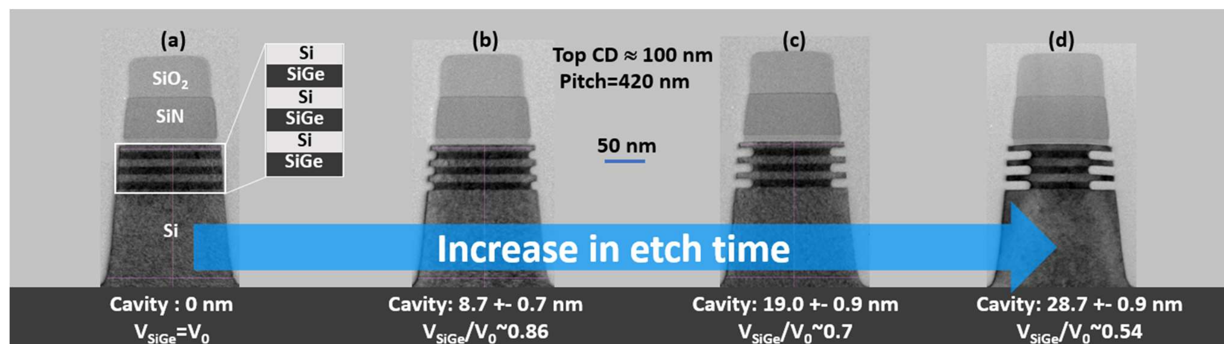

Figure 1. Transmission electron micrographs of the samples used in this paper, i.e. 100-nm wide fins including a 6-layer $Si_{75}Ge_{25}$/Si superlattice covered with a SiO_2/SiN/SiO_2 hard mask. The depth of the cavities ranges from 0 to 28.7 nm. The used target has a 420 nm pitch and a 250 μm fin length.

Note that these samples do not include the dummy gate normally present on top of the fins at the cavity etch step[7]. However, the 100-nm thick hard mask nicely emulates the gates and allows to maintain the full complexity of the measurement of such buried information.

3. CONVENTIONAL CD METROLOGY

In this Section, we evaluate the sensitivity of commonly used dimensional metrology techniques to the cavity depth and evaluate how this sensitivity could be improved. First, as we show in Section 3.1, SEM is insensitive to buried information due to the low landing energy usually used to maximize the sensitivity to topography of the top layer and minimize the influence of underlayers[8]. However, as we show theoretically, an increased landing energy could lead to an improved sensitivity to cavity depth. Second, Section 3.2 demonstrates that AFM also lacks sensitivity to cavity depth due to the limited information AFM can provide on fin sidewalls. Tilting the AFM tip mitigates that problem but requires wide spacings between the fins and anyway results in very limited maximum probing cavity depth. Finally, OCD proves to be very sensitive to cavity depth. However, the technique requires a model of which the complexity increases as the device geometry gets more sophisticated[6] and is therefore not very intuitive. Furthermore, correlations between the different geometrical parameters may occur. These correlations could be broken by adding independent information, e.g. from one of the techniques introduced in Section 4.

Downloaded From: https://www.spiedigitallibrary.org/conference-proceedings-of-spie on 23 Feb 2021
Terms of Use: https://www.spiedigitallibrary.org/terms-of-use

3.1 SEM

SEM is the most common technique for measuring the width and edge roughness of nanometer-wide lines[8]. This imaging technique is based on the measurement of the secondary and/or backscattered electrons collected locally while scanning a nanoscale electron beam across the sample surface[9]. Its nanometer lateral resolution would make it the ideal candidate for cavity depth measurements.

Unfortunately, to maximize the sensitivity to surface topography, most inline SEM tools use low (~0.2-0.6 keV) landing energies, which results in limited probing depth[8]. This is confirmed by Figs. 2(a) and (b) where no differences are observed between two SEM images taken at 0.2 keV landing energy on samples with respective cavity depths of 15 nm and 30 nm. This is also theoretically shown in Fig. 2(c) where even a 1 keV landing energy leads to no more than 2 nm depth of maximum electron backscattering, i.e. depth of maximum sensitivity. This figure was obtained from Monte Carlo simulations using the Casino program[10] assuming the stack of Fig. 1.

Interestingly, Fig 2(c) also shows that, at landing energies ranging from ~6 keV to ~13 keV, electrons can reach and backscatter on the buried SiGe/Si superlattice. Besides, the mass of the Ge atom being the heaviest of the full stack ensures a high backscattering efficiency on SiGe, which should provide a high sensitivity to the latter layers[9]. In other words, SEM might remain an interesting technique for cavity depth metrology, but high landing energies unavailable in most inline tools, are required.

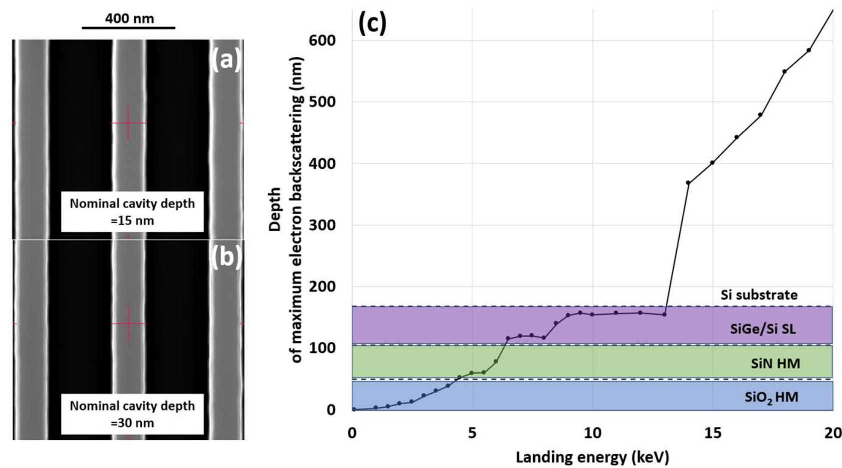

Figure 2. (a),(b) SEM images obtained at 0.2 keV landing energy on samples with respective cavity depths of 15 nm and 30 nm. No clear difference is observed between the two images indicating the lack of sensitivity of low landing energy SEM to cavity depth. (c) Theoretically calculated increase in depth of maximum electron backscattering, i.e. of maximum sensitivity, with increasing electron landing energy on the stack of Fig. 1 according to Monte Carlo simulations using the Casino program[10].

3.2 AFM

In AFM, a nm-sharp tip mounted on a soft cantilever is scanned across the sample surface to probe its topography[11]. The technique relies on the interaction between the tip apex and the surface, which bends the cantilever up and down as the tip follows the surface topography. The lateral resolution when measuring the CD of a line is limited by the size of the tip apex (>~ 10 nm) which interacts with the surface. In the direction perpendicular to the surface, the resolution is much higher (<1 nm) as the vertical movements of the tip are recorded very precisely from the change in position of a laser spot reflected off the bent cantilever[11]. In other words, to probe the depth of a cavity, the AFM tip should ideally be placed perpendicular to the fin sidewall.

It is thus no surprise that, in Fig. 3(a), the AFM scan measured with the tip perpendicular to the wafer surface (red curve) offers no information about the fin sidewalls or the cavities. Note e.g. the underestimated verticality of the sidewall vs the overlaid TEM. As the tip scans the fin sidewall, the tip sidewall also interacts with the fin[12]. What is measured is therefore a convolution of the fin and tip sidewalls, which leads to a virtually complete loss of sensitivity.

Downloaded From: https://www.spiedigitallibrary.org/conference-proceedings-of-spie on 23 Feb 2021
Terms of Use: https://www.spiedigitallibrary.org/terms-of-use

On the other hand, as the tip is scanned with a tilt angle of 38° (green curve), the observation of the sidewall and the cavities corresponds more accurately to the structure as observed by comparison with the overlaid TEM. This confirms that tilting the tip allows to extract useful and precise information about the sidewall topography. However, it can also be seen in Fig. 3(b) that AFM has limited probing depth and cannot discriminate the 15 nm and 30 nm cavity depths. Furthermore, we also observe in Fig. 3(a) that tilted AFM cannot probe the full height of the fin. At the bottommost point, the tip sidewall is in contact with the next fin located ~320 nm to the left. This is not a major issue in the considered case because the pitch is very relaxed (420 nm). However, if the pitch was reduced to ~200 nm or lower, the bottommost point will move up such that the tip would no longer be able to access the cavities.

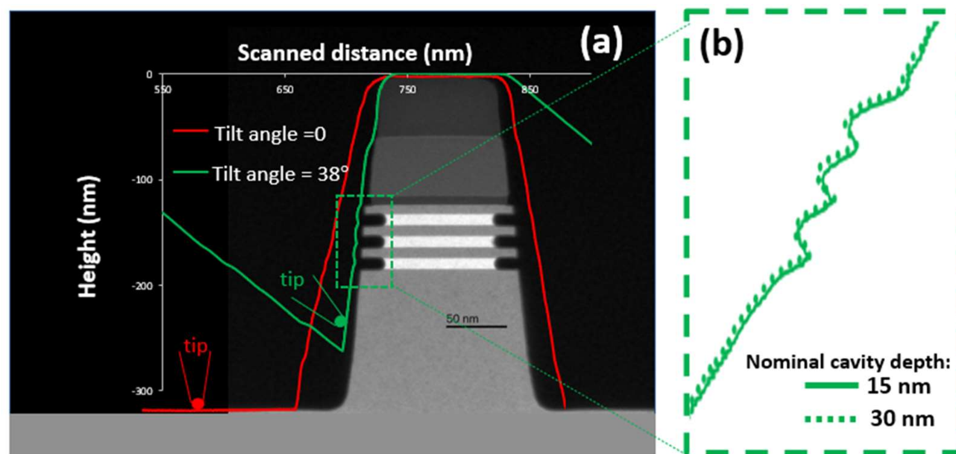

Figure 3. (a) overlay of a TEM representative of our samples with 2 AFM scans run respectively without tilt (red) and with 38° tilt angle (green). Only the tilted AFM scan can access information about the fin sidewall and the cavities. (b) Zoom on the tilted AFM scans in the region of the cavities. Tilted AFM can sense the presence of the 3 cavities but not the difference in cavity depth between the 2 samples (15 vs 30 nm).

In summary, zero-tilt AFM is not suited for cavity depth measurements as it is insensitive to information along the fin sidewalls. Tilted AFM, on the other hand, does sense the cavities but with a limited probing depth and only on structures with a relaxed pitch.

3.3 OCD

In OCD, the reflectivity of a periodically repeated array of the structures to be characterized is measured under different illumination conditions, i.e. different wavelengths, polarizations, angles of incidence and azimuths. The different measured reflectivity spectra (see e.g. Fig 4(a)) are then fitted by solving Maxwell's wave equation using the Rigorous Coupled Wave Analysis technique[12] on a geometrical model such as shown in Figs 4(b) and (c). Beyond the geometrical parameters, the required input for the latter model are the optical indices (n,k) of all involved materials.

Fig. 4(a) shows the sensitivity to cavity depth of the normal-incidence spectra measured with the NOVA T600MMSR on the two samples with respective nominal cavity depths 15 nm (full lines) and 30 nm (dashed lines) respectively with transverse electric (TE, red) and transverse-magnetic (TM, blue) polarizations. As observed, the TE channel shows higher sensitivity to the cavity depth over virtually the full spectral range compared to TM. This is expected as TE-polarized light is known to propagate within the fins in such periodic arrays [13,14]. TM-polarized light, on the other hand, tends to propagate in the spacer (i.e. air) and is therefore little impacted by a change in cavity depth[13].

Figs. 4(b) and (c) show the profiles of the samples with respectively 15 and 30 nm cavity depths based on the fitting of the spectra of Fig. 4(a) (small circles) using the NOVA MARS software package[15]. As can be observed, the fitted cavity depth values of 13 and 28 nm, as well as the overall profile shape, are very close to what is nominally expected. This shows the amazing power of OCD, i.e. its ability to predict the full geometry of the measured device (here 9 geometrical parameters) in a <1-min long non-contact measurement. However, these figures also show two of the difficulties faced by OCD. First

Downloaded From: https://www.spiedigitallibrary.org/conference-proceedings-of-spie on 23 Feb 2021
Terms of Use: https://www.spiedigitallibrary.org/terms-of-use

and foremost, OCD is sensitive to the complete geometry of the device, i.e. including parameters which might be of little relevance. In some cases, correlations between these parameters may exist, which leads to non-unique solutions and therefore requires complex injection strategies[6]. Second, OCD is model-based, hence indirect and not intuitive. This is also a consequence of the wealth of information contained in the OCD spectra.

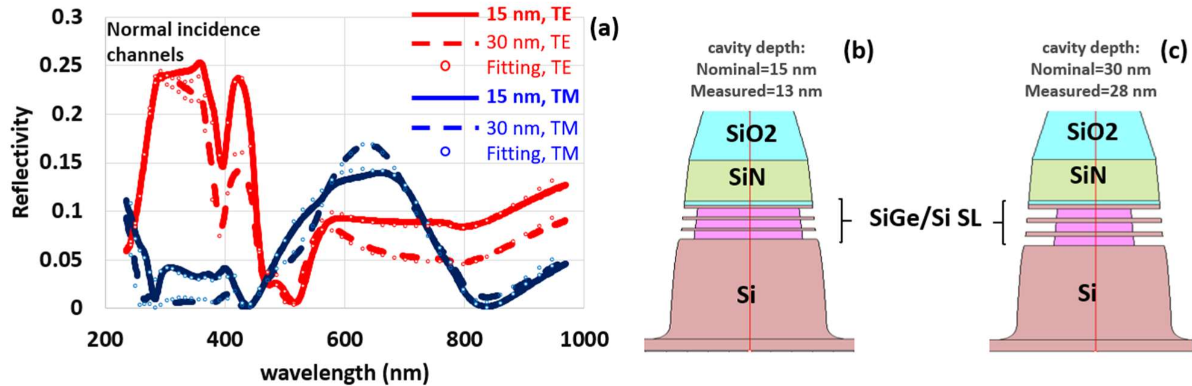

Figure 4. (a) Normal-incidence reflectivity spectra measured on two samples with respective nominal cavity depths 15 nm full lines) and 30 nm (dashed lines) with respectively transverse-electric (TE, red) and transverse-magnetic (TM, blue) polarizations. Strong sensitivity to cavity depth is observed mostly with TE polarization (red). (b) and (c) Reconstructed profiles of the samples with respectively 15- and 30-nm nominal cavity depths based on the fitting of the spectra of (a).

In summary, OCD is very close to fulfilling the need for fast inline characterization of cavity depth. However, this technique being indirect and sensitive to so many geometrical parameters, it would deeply benefit from extra independent input from other techniques which are more direct/intuitive and less sensitive to the full device geometry.

4. CD METROLOGY BASED ON TOP-DOWN SPECTROSCOPIC TECHNIQUES

As we showed in Section 3, conventional CD metrology lacks sensitivity to cavity depth and/or would benefit from extra information coming from more direct and intuitive techniques. In this Section, we first introduce the idea behind the use of top-down spectroscopic techniques for cavity depth measurements. Next, we evaluate the sensitivity and capabilities for such measurements of EDX (Section 4.1), Raman spectroscopy (Section 4.2), XPS (Section 4.3) and SIMS (Section 4.4). As we will demonstrate experimentally, these techniques simply measure the volume of SiGe remaining under the beam.

The idea behind the use of spectroscopic techniques for cavity depth measurements is explained in Fig. 5(a). Irrespective of the technique, an excitation beam impinges top-down on a periodic array of the devices to be characterized. The interaction between the sample and the beam results in the emission of a secondary beam. The excitation and emitted beams can both be made up of electrons, photons or ions, according to the considered spectroscopic technique. If measured with an energy- or mass-sensitive detector, the emitted beam will reveal several peaks at energies/masses representative of the different materials or elements constituting the stack. As discussed mathematically below, the integral under these peaks is a measure of the volume of the considered material/element present under the excitation beam. In other words, a loss of volume will result in a reduced peak height. This is precisely what is observed in Fig. 5(b) where the drop in integrated signal for a deeper cavity is overlaid for the four techniques. The latter figure is of critical importance as it experimentally demonstrates the value of using these top-down spectroscopic techniques for cavity depth measurements.

To clarify the sensitivity which can be expected from spectroscopic techniques, let us give a simple mathematical description of the signals measured on the samples described in Fig. 1. If we assume a uniformly excited volume V_{SiGe}, the

Downloaded From: https://www.spiedigitallibrary.org/conference-proceedings-of-spie on 23 Feb 2021
Terms of Use: https://www.spiedigitallibrary.org/terms-of-use

integrated intensity $S_{integrated}$ under the peak representative of SiGe material simply varies linearly with V_{SiGe} (see e.g. eq. (2.14) of Ref. [9]), i.e.

$$S_{integrated} = \alpha V_{SiGe} = \alpha \times N_{fins} \times (W_{SiGe} - d_{cavity}) \times (3 \times t_{SiGe}) \times D_{beam}, \quad (1)$$

where α is a proportionality factor dependent on the considered technique and input parameters such as incident power, integration time etc. D_{beam} is the excitation beam diameter, N_{fins} is the number of fins under the excitation beam ($=D_{beam}$/pitch), W_{SiGe} is the fin width at the level of the SiGe layers, d_{cavity} is the cavity depth, and $3 \times t_{SiGe}$ is the total thickness of the 3 SiGe layers. Two assumptions were needed to derive eq. (1). First of all, vertical fin sidewalls were assumed. Second and most importantly, the full SiGe volume was assumed uniformly excited. Yet, the intensity of the incident beam typically decreases exponentially as it travels from the top surface deeper down into the sample as a result of multiple interactions (absorption, scattering,...). Furthermore, a non-uniform lateral distribution of the incident intensity may also be expected in the patterned samples of Fig. 1. Consequently, the intensity of the peak representative of the SiGe material is actually proportional to a convolution of V_{SiGe} with the distribution of the incident beam intensity inside the SiGe volume[9]. We propose below a first-order correction for this assumption.

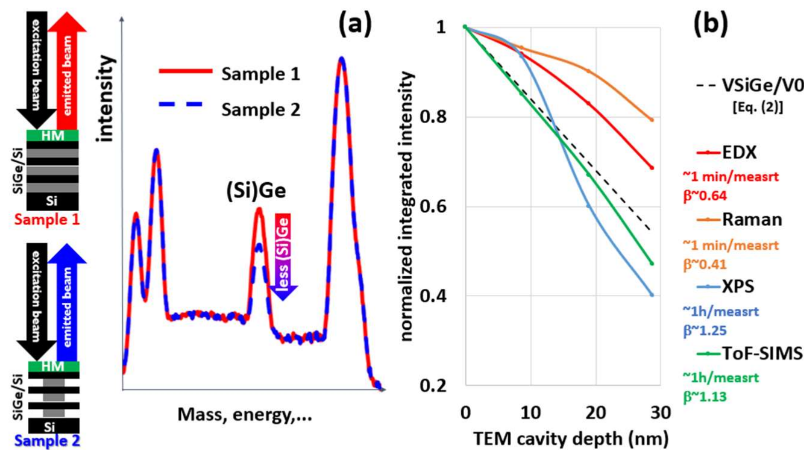

Figure 5. Cavity depth measurements with top-down spectroscopic techniques. (a) A primary beam of electrons, photons or ions impinges top-down and excites the sample to be characterized. This interaction leads to the emission of a secondary beam of electrons, photons or ions. One specific peak of the mass- or energy-resolved emitted beam is representative of the volume of SiGe volume present under the excitation beam. The peak intensity therefore drops as the cavity is etched deeper (b) Summary of the experimental results obtained with the four considered top-down spectroscopic techniques, indicating their sensitivity to the loss in SiGe volume V and the approximate measurement time.

Eq. (1) already shows one of the values of such spectroscopic techniques, i.e. they are direct and intuitive. It is indeed easy to see with eq. (1) that, the integrated signal will drop monotonically as the material is etched. Second, it is simple to predict that cavity depth measurements will face geometrical correlations with e.g. t_{SiGe} and W_{SiGe}.. We leave the question of whether these correlations can be easily broken or not, i.e. whether the proposed techniques can be used as stand-alone techniques or not, for future discussions.

If we further assume that all the samples of Fig. 1 have identical geometries except for the cavity depth, normalizing eq. (1) to the integrated signal S_0 on the unetched sample yields the normalized integrated intensity $S_{normalized}$, i.e.

$$S_{normalized} = \frac{S_{integrated}}{S_0} = \frac{V_{SiGe}}{V_0} = 1 - \frac{d_{cavity}}{W_{SiGe}} \quad , \quad (2)$$

where V_0 is the SiGe volume of the unetched sample. The behavior of eq. (2) is represented by the black dashed line in Fig. 5(b). Unfortunately, as mentioned above, in most tested techniques, the SiGe volume is not uniformly excited such that the experimentally observed behavior does not overlay with eq. (2). As a tentative simplified equation accounting for the non-uniform volume excitation, we write

$$S_{normalized} = 1 - \beta \times \frac{d_{cavity}}{W_{SiGe}} \quad , \quad (3)$$

Downloaded From: https://www.spiedigitallibrary.org/conference-proceedings-of-spie on 23 Feb 2021
Terms of Use: https://www.spiedigitallibrary.org/terms-of-use

where β is a sensitivity factor incorporating the impact of non-uniform excitation. Fig. 5(b) confirms that eq. (3) acceptably models the measured data. The β values indicated for the different techniques were obtained by linearly fitting the experimental data of Fig. 5(b) with eq. (3). In the next Sections, more information and discussion will be given on the plotted signals and on the possible optimization of the sensitivity factor β for each respective technique.
As a final note, let us mention that all the measurements of this Section were actually obtained on laboratory-based tools. However, the chosen spectroscopic techniques also exist as fully automated fab-based platforms. Variations with the laboratory tools we have used may of course exist but are not discussed here.

4.1 EDX

In EDX, also called electron microprobe, the excitation beam is composed of electrons while the emitted signal consists of X-rays[9,16] (Fig. 6(a)). As the primary electron beam travels through the structure, inner shell electrons of the different elements reached by the primary electrons are kicked out of their energy levels as secondary electrons. As electrons subsequently relax and fill the left-empty energy levels, X-ray photons are emitted with an energy representative of the element which they originate from[9,16].

Fig. 6(b) shows the EDX spectra measured with an Xl 31 nanoprober tool from Oxford Instruments on the sample of Fig. 1(a) with different landing energies. The different characteristic peaks for Si, N, O and most importantly Ge are indicated. Our data show that an electron landing energy of 5.7 keV (green) is close to optimal for reaching the SiGe/Si superlattice and ionize the Ge atoms. At 3 keV landing energy (blue), the absence of a Ge Lα peak (at 1.2 keV) indicates that ionization has only taken place in the SiO_2/SiN hard mask while at 10.4 keV landing energy (red), most of the incident energy is lost in the Si substrate and the sensitivity to the Ge content drops.

Most importantly, Fig. 6(c) shows that the Ge Lα peak intensity drops significantly as the cavity is etched from 0 nm to 28.7 nm. This demonstrates the good sensitivity of the technique to cavity depth. Unfortunately, this figure also shows one of the drawbacks of EDX, i.e. a large background is observed on the Ge Lα peak. The background in EDX is mostly due to bremsstrahlung X-rays[9] and can therefore not be eliminated experimentally. As a result, EDX has a relatively poor limit of detection and will not be useful for e.g. measurement of SiGe traces (nanosheet release[2,5]).

After integration of the surface under the Ge peak and background removal on the measurements run on all four samples of Fig. 1, the complete sensitivity curve for EDX is shown in Fig. 5(b) (red). From this figure, it is obvious that EDX is a good choice for minute-long non-destructive and non-contact cavity depth measurement. Furthermore, the obtained β value (β~0.64) could still be enhanced with a laterally more uniform excitation of the SiGe volume, i.e. on devices with a smaller width or by increasing the excitation beam radius. The former solution is anyway what is found in all state-of-the-art devices where CD<~20 nm[7].

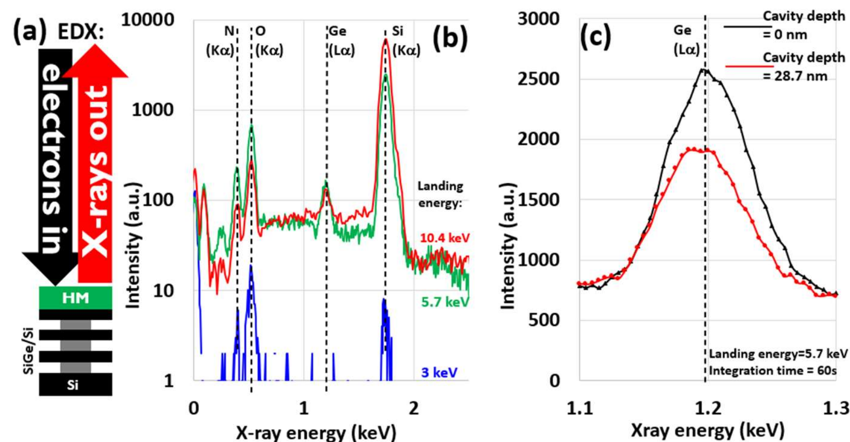

Figure 6. (a) Principle of EDX. (b) EDX spectra of the sample with cavity depth = 0 nm measured at different landing energies. The Ge Lα peak at 1.2 keV is optimally resolved at a landing energy = 5.7 keV. (c) The Ge Lα peak intensity drops as the SiGe is etched from 0 nm to 28.7 nm cavity depth, which demonstrates the sensitivity of EDX to cavity depth.

Downloaded From: https://www.spiedigitallibrary.org/conference-proceedings-of-spie on 23 Feb 2021
Terms of Use: https://www.spiedigitallibrary.org/terms-of-use

4.2 Raman spectroscopy

In Raman spectroscopy, both the excitation beam and emitted signal are composed of photons[16] (Fig. 7(a)). However, the wavelength of the emitted beam in this nonlinear optical technique is shifted after scattering of the excitation beam and emission/annihilation of phonons within the illuminated structure. This change in wavelength, i.e. the Raman shift, is a measure of the phonon energy which is directly linked to bond strength within the material. For this reason, Raman spectroscopy is commonly used for measurement of e.g. stress and composition in blanket but also patterned semiconductor srtructures[17,18].

Fig. 7(b) shows the Raman spectra measured with the Horiba Jobin-Yvon HR800 Raman tool on the sample of Fig.1(a) with different incident wavelengths. Two peaks are observed at respectively 510 and 520 cm^{-1}, which are attributed to scattering with the Si-Si bond vibration respectively in SiGe and in Si. This difference in peak position can be understood as reflecting the less energetic bond (larger lattice constant) in SiGe than in Si[19]. As can also be observed in Fig. 7(b), a shorter incident wavelength leads to a better resolved SiGe peak. This is due to the smaller penetration depth at a shorter wavelength[20], which thus enhances the visibility of the SiGe peak vs the dominant Si peak. Finally, it is also important to mention that incident TE polarization, i.e. electric field parallel to the fin, is required for such measurements as it ensures that most of the electric field penetrates into the fin[13,14]. Conversely, TM polarization leads to light propagating inside the spacer, i.e. air, and therefore to low intensity SiGe peaks (not shown).

Quite surprisingly, as Fig. 7(c) shows, while only a reduction in the SiGe peak might have been expected, a rise in both the Si and SiGe peaks was obtained as the SiGe is etched. The overall increase across the measured spectrum means that the electric field within the fin has been enhanced when etching SiGe. However, the Si peak rises faster than the SiGe peak, i.e. the sensitivity to cavity depth is present. The overall rise in the measured spectrum is the combined effect of a reduction in both the reflectivity and the absorptivity of the sample, as confirmed in the OCD data of Fig.4 (a) and by finite-element simulations (not shown).

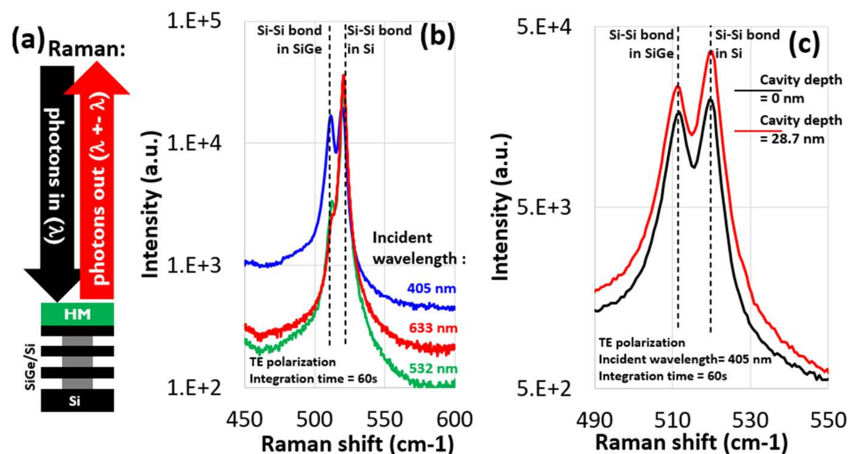

Figure 7. (a) Principle of Raman spectroscopy. (b) Raman spectra of the sample with cavity depth = 0 nm measured at different incident wavelengths. While the peak at 520 cm^{-1} Raman shift is characteristic of Si, the peak at 510 cm^{-1} is characteristic of SiGe and is optimally resolved at an incident wavelength = 405 nm. (c) Both the peaks at 520 cm^{-1} (Si) and at 510 cm^{-1} (SiGe) increase as the SiGe is etched from 0 nm to 28.7 nm cavity depth. However, the ratio of the two peaks indicates a reduction of the SiGe content vs Si, which demonstrates the sensitivity of Raman spectroscopy to cavity depth.

To account for the field enhancement as the etch proceeds, the Raman signal we opted for and plotted in Fig. 5(b) is the ratio of the integrated SiGe and Si peaks. As observed, this ratio monotonically decreases as the SiGe is etched, which demonstrates the value of Raman as minute-long non-destructive and non-contact cavity depth measurement technique. However, Raman has the smallest sensitivity factor (β~0.41) of all four shown techniques. This is due to a very non-uniform electric field distribution within our wide pitch structure. As Ref. [14] shows, the electric field becomes much

Downloaded From: https://www.spiedigitallibrary.org/conference-proceedings-of-spie on 23 Feb 2021
Terms of Use: https://www.spiedigitallibrary.org/terms-of-use

more uniform laterally (~plane wave) as the pitch and CD are scaled down. It is therefore expected and has been confirmed experimentally that the sensitivity factor approaches unity on 90-nm pitch structures (not shown).

4.3 XPS

XPS is based on the photelectric effect[16]. A beam of monochromatic X-ray with energy $E_{X\text{-ray}}$ ionizes the elements present in the sample by kicking out inner shell electrons, which exit the sample forming a photoelectron signal (Fig. 8(a)). The photoelectrons are emitted with a kinetic energy $E_{e-}=E_{X\text{-ray}}-E_{binding}$, where the binding energy is material-specific[16].

At first sight, the relevance of XPS for measuring buried information is questionable. Indeed, as the energy equation above suggests, the exit kinetic energy E_{e-} of the electrons is upper-bounded by the incident energy $E_{X\text{-ray}}$, which for incident Al Kα is $E_{X\text{-ray}}$=1.4866 keV. In other words, the photoelectrons are emitted with a low kinetic energy, resulting in limited escape depth and hence depth of probing, as already discussed in Sections 3.1 and 4.1 in the context of SEM and EDX respectively. Interestingly, variants of XPS such as hard X-ray photoelectron spectroscopy (HAXPES), in which incident Cr Kα ($E_{X\text{-ray}}$= 5.4149 keV) or Ga Kα ($E_{X\text{-ray}}$= 9.2248 keV) photons are used, lead to probing depths up to a few 10s of nanometers[21].

In this paper, we still used conventional XPS, i.e. Al Kα photons incident parallel to the lines to avoid any lateral shadowing effects[22]. Given the limited probing depth of XPS, we removed the thick hard mask on top of the SiGe/Si superlattice and expose the top Si layer, as schematically shown in Fig 8.(a). Fig. 8(b) shows the Ge3d peak as measured with the QUANTES instrument from Physical electronics on the 4 samples of Fig. 1. As expected, a drop in Ge3d peak is observed as the SiGe is laterally etched. This figure shows the sensitivity of XPS to cavity depth and Fig. 5(b) summarizes the results after integration and normalization of the peaks. As observed, the normalized integrated XPS signal drops quickly as the cavity etch proceeds but the drop does not follow the expected linearity of eq. (3). We understand this non-linearity as being due to the high sensitivity of XPS to any change in surface oxidation and/or in thickness of the top Si layer after HM etch.

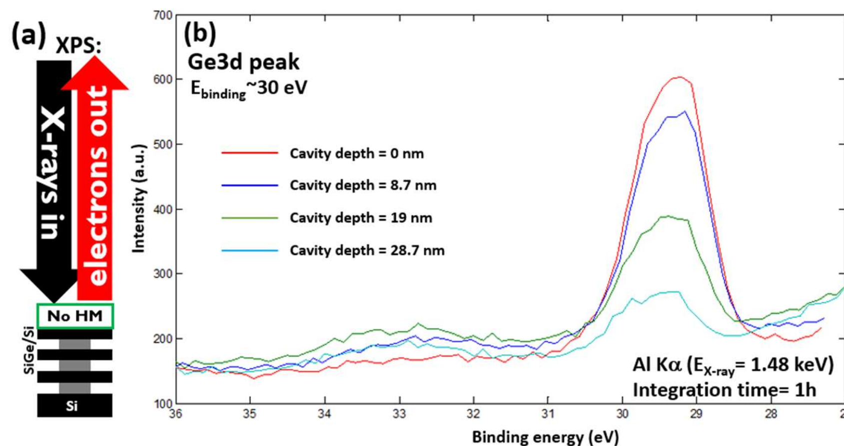

Figure 8. (a) Principle of XPS on a sample without a hard mask (b) Drop in intensity of the Ge3d peak as the SiGe is etched in the samples of Fig. 1.

To conclude, XPS shows a very interesting sensitivity to cavity depth but it also comes with three critical weaknesses. First of all, the probing depth is limited although, as mentioned, the use of hard X-rays can alleviate this issue. Second, the typical measurement time is quite significant (~1 hour/sample). However, both these weaknesses are somewhat mitigated

Downloaded From: https://www.spiedigitallibrary.org/conference-proceedings-of-spie on 23 Feb 2021
Terms of Use: https://www.spiedigitallibrary.org/terms-of-use

in in-line XPS tools using a higher incident X-ray fluence. Third, and most important of all, XPS is very sensitive to surface oxidation and to variations in the thickness of the layers covering the SiGe/Si superlattice. This leads to very strong correlations which we believe will be hard to break.

4.4 SIMS

In SIMS, a primary ion beam collides with the sample and sputters its top surface[16] (Fig 9(a)). The ionized species sputtered from the sample form a secondary ion beam which is accelerated and analyzed in a mass-sensitive detector. We used the TOF-NCS tool of ION-TOF GmbH, wherein the detection is ensured by a time-of-flight (ToF) detector[16]. This tool has a dual beam configuration, where two separate beams are used to respectively sputter and analyze the sample. In this paper, we used a Cs+ (350 eV) and a Bi1+ (30 keV) beams respectively for sputtering and analysis, both being incident at a 45° angle along the fins to avoid any shadowing[22].

One of the principal advantages offered by SIMS lies in its depth-profiling capabilities, as exemplified in Fig. 9(b) for the sample of Fig.1(a). While measuring, the sample is indeed sputtered and analyzed layer by layer. This leads to a wealth of information, where the subsequent regions (see the different colors for SiO_2, SiN, superlattice and substrate in Fig 9(b)) and even the 3 SiGe layers of the superlattice are easily recognized. Furthermore, as also observed, SIMS has a very wide dynamic range and a very low detection limit. Notice e.g that the Ge^- signal varies almost 3 orders of magnitude along the profile while keeping the noise level very low. This makes SIMS a very promising technique for depth profiling of cavities with a precision allowing to go down to SiGe residue during nanosheet release. Finally, as shown in Figs. 9(c), (d) and (e), SIMS is also very sensitive to cavity depth and even offers sensitivity via different ion channels, i.e. respectively Ge^-, $SiGe^-$ and Ge_2^-. On top of it, after integration of the Ge- profiles on all four samples, SIMS is shown to offer a very good sensitivity to cavity depth, i.e. $\beta \sim 1.13$ (Fig. 5(b)).

Nonetheless, two critical drawbacks of SIMS must be mentioned. First and foremost, the technique is inherently destructive as it is based on sputtering. Second, it is time-consuming (~1 hour/measurement). However, the latter measurement time can be dramatically reduced if the need for depth profiling is relaxed. Indeed, we have also used high-energy (>1 kV) sputtering beams to reduce the measurement time to <1 min while keeping the good sensitivity factor (not shown). However, this only gave access to the integrated remaining SiGe volume in the sample, similar to the other spectroscopic techniques of this paper.

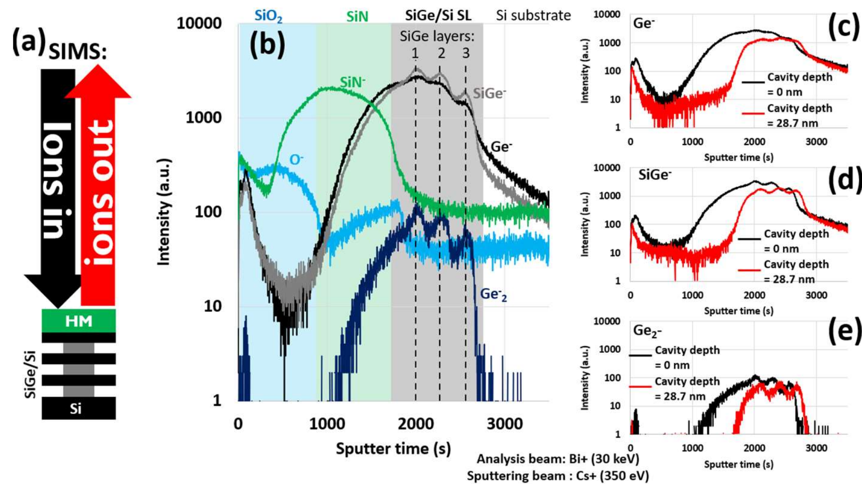

Figure 9. (a) Principle of SIMS. (b) SIMS depth profile of the sample of Fig. 1(a). As the sputter time proceeds, information from different depths is obtained, allowing e.g. to look at the three SiGe layers separately. (c),(d) and (e) Three measured ions, i.e. respectively Ge^-, $SiGe^-$ and Ge_2^-, contain information about the Ge, i.e. their intensity drops as the etch proceeds from 0 nm to 28.7 nm.

Downloaded From: https://www.spiedigitallibrary.org/conference-proceedings-of-spie on 23 Feb 2021
Terms of Use: https://www.spiedigitallibrary.org/terms-of-use

5. CONCLUSION

In this paper, we have shown that the CD metrology techniques typically found in fabs, i.e. SEM, AFM and OCD either lack sensitivity to buried cavity depth and/or would benefit from independent information obtained from another technique. Subsequently, we have proposed to use top-down spectroscopic techniques such as EDX, Raman, XPS and SIMS for fast inline cavity depth measurements. As we showed, all four techniques are sensitive to the remaining SiGe volume inside the sample, thus giving intuitive information about the depth of the buried cavities. Suggestions for improvement of the sensitivity of each technique have also been given. A comparison of all the evaluated techniques can be found in Table 1.

Table 1. Comparison of the different techniques considered in this paper for cavity depth measurements.

Technique / Feature	SEM	AFM	OCD	EDX	Raman	XPS	SIMS
Excitation beam	e-	N/A	light	e-	light	X-ray	ions
Emitted beam	e-	N/A	light	X-ray	light	e-	ions
Lateral sampling size	~ nm	~ nm	~25 µm	~100 nm	>=1 µm	>=50 µm	>=50 µm
Device vs array sampling	single device	single device	array	device or array	array	array	array
Measurement time	< 1 min	~ hour	< 1 min	~ 1 min	~ 1 min	Min-hour	Min-hour
Sensitivity to cavity depth	High landing energy required	Tilt and wide pitch required	Possible correlations	$\propto$ Volume of SiGe	$\propto$ Volume of SiGe	$\propto$ Volume of SiGe	$\propto$ Volume of SiGe
Non-contact, Non-destructive						Hard mask removal required	Inherently destructive

REFERENCES

[1] J. Ryckaert, imec magazine, pp. 14-19, December 2019.
[2] Y. Oniki et al., ECS Trans., 92, 3 (2019).
[3] A. Veloso et al., ECS Transactions 97(5):3-14 (2020)
[4] N. Loubet et al., IEDM Tech. Dig., 242 (2019).
[5] S. Kal et al., Proc. SPIE, 10963 (2019).
[6] A.-L. Charley et al., Proc. SPIE, 1058505 (2018)
[7] H. Mertens et al., VLSI Tech. Dig., 158 (2016)
[8] G. Lorusso et al., Jpn. J. Appl. Phys. 58 SD0801 (2019)
[9] N. Chatterjee. 12.141 Electron Microprobe Analysis. January IAP 2012. Massachusetts Institute of Technology: MIT OpenCourseWare
[10] https://www.gel.usherbrooke.ca/casino/index.html
[12] B. Bhushan, H. Fuchs, M. Tomitori, Applied Scanning Probe Methods VIII, Chap. 2, Springer (2008)
[12] A. Diebold, Handbook of Silicon Semiconductor metrology, Chap. 18, Taylor & Francis (2005)
[13] J. Bogdanowicz et al., Applied Physics Letters 108, 083106 (2016)
[14] A. Gawlik et al., Appl. Phys. Lett. 113, 063103 (2018)

Downloaded From: https://www.spiedigitallibrary.org/conference-proceedings-of-spie on 23 Feb 2021
Terms of Use: https://www.spiedigitallibrary.org/terms-of-use

[15] https://www.novami.com/nova-product/novamars/
[16] D.K. Schroder, Semiconductor Material and Device Characterization, Chap. 11, Wiley (2006)
[17] I. De Wolf, J. Appl. Phys. 71 898 (1992)
[18] T. Nuytten et al., APL Mat 6 058501 (2018)
[19] F. Pezzoli et al., Journal of Applied Physics 103, 093521 (2008)
[20] J. G. E. Jellison and F. A. Modine, Appl. Phys. Lett 41, 180-182 (1982)
[21] S. Siol, Surf Interface Anal, 1–9 (2020)
[22] S. Hajati & S. Tougaard, Anal Bioanal Chem 396,2741–2755 (2010)

Downloaded From: https://www.spiedigitallibrary.org/conference-proceedings-of-spie on 23 Feb 2021
Terms of Use: https://www.spiedigitallibrary.org/terms-of-use